UKAEA-CCFE-CP(20)124

Chantal Nobs, Jonathon Naish, Lee Packer, Mario Pillon, Maurizio Angelone, Stefano Loreti, Paolo Del Prete, Jesus Izquierdo, Raul Pampin, Luca Zanibellato

Computational evaluation of N-16 and N-17 measurements for a 14 MeV neutron irradiation of an ITER first wall component with water circuit

Computational evaluation of N-16 and N-17 measurements for a 14 MeV neutron irradiation of an ITER first wall component with water circuit

Chantal Nobs, Jonathon Naish, Lee Packer, Mario Pillon, Maurizio Angelone, Stefano Loreti, Paolo Del Prete, Jesus Izquierdo, Raul Pampin, Luca Zanibellato

This paper has been submitted to
14th International Symposium on Fusion Nuclear Technology (ISFNT-14) Budapest,Hungary, 22-27 September 2019

Computational evaluation of N-16 measurements for a 14 MeV neutron irradiation of an ITER first wall component with water circuit

C.R. Nobs[a,*], J. Naish[a], L.W. Packer[a], R. Worrall[a], M. Angelone[b], A. Colangeli[b], S. Loreti[b], M. Pillon[b], R. Villari[b]

[a] *Culham Centre for Fusion Energy, Culham Science Centre, Abingdon, Oxon, OX14 3DB, UK*
[b] *ENEA - Department of Fusion and Technology for Nuclear Safety and Security via E. Fermi 45, 00044 Frascati (Rome), Italy*

Abstract

During ITER operations the water coolant flowing through components such as the first wall, blanket modules, divertor cassettes and vacuum vessel will become activated by high energy neutrons. Two key neutron-induced reactions will occur with oxygen in the water producing the radioactive isotopes N-16 and N-17, which have relatively short half-lives of a few seconds. These nuclides are transported in coolant loops and, unmitigated, their decay emissions will induce additional nuclear heat in components, potentially including superconducting magnets, and lead to an increase in the occupational dose for workers and sensitive equipment outside the biological shield. Variations in irradiation, water flow rate and cooling circuit parameters make it difficult to predict nuclear heating. A water activation experiment has recently been performed at the 14 MeV Frascati Neutron Generator to accurately measure N-16 and N-17 produced by irradiating an ITER first wall mock-up. This experiment aimed to validate the methodology for water activation assessment used for ITER and to provide scientific justification to reduce safety factors, which have a large impact on ITER component design and qualification. This paper provides a detailed description of neutronics calculations performed using the GammaFlow code to model the temporal evolution of activated water, along with MCNP6.1 and FISPACT-II to calculate the detector response. The calculated reaction rates associated with nuclear data from ten libraries have been compared with measured data, although as many cross-sections originated from the same library effectively five nuclear data libraries have been compared.

Keywords: neutronics, neutron detector, FNG, unfolding, neutron activation

1. Introduction

The water coolant in ITER components such as those inside the first wall, blanket modules, divertor cassettes and vacuum vessel will become activated by neutrons during D-T plasma operations. Two key neutron induced reactions will occur with oxygen producing the radioactive nitrogen isotopes N-16 and N-17 through the following reactions:

$$^{16}\mathrm{O(n,p)}^{16}\mathrm{N} \rightarrow\ ^{16}\mathrm{O} + \gamma, \quad (1)$$

$$^{17}\mathrm{O(n,p)}^{17}\mathrm{N} \rightarrow\ ^{17}\mathrm{O} \rightarrow\ ^{16}\mathrm{O} + \gamma, \quad (2)$$

Reaction 1 produces gamma rays at 6.13 MeV (gamma emission probability per disintegration, I=67%) and 7.12 MeV (I=5%), whereas reaction 2 produces delayed neutrons at 0.386 MeV (I=37.7%), 0.886 MeV (I=0.6%), 1.16 MeV (I=49.8%), 1.69 MeV (I=6.9%) and gammas at 0.87 MeV (I=3.7%) [1, 2]. Because water coolant is being pumped and transported to other locations, the decay emissions from these nuclides will induce nuclear responses in sensitive tokamak and plant components, e.g. nuclear heat in superconducting magnets, absorbed doses in polymer-based components like valves or high dose rates in electronics. The uncertainty in the calculation of radiation maps due to activated water is evaluated to be very large [3, 4], the main sources of uncertainty being due to modelling (~200%) and nuclear data, and hence safety factors between 8.2 and 4.7 are applied. The motivation for this new experiment is to accurately measure the N-16 and N-17 in an ITER-like environment with the aim to validate the methodology for water actvitation assessment used for ITER and provide a scientific justification to reduce these safety factors.

*Corresponding author
Email address: `chantal.nobs@ukaea.uk` (C.R. Nobs)

2. Experimental Setup

The ITER first wall (FW) mock-up was placed at two distances, 5 cm and 2 cm, from the Frascati Neutron Generator (FNG) 14 MeV neutron source target and connected to a water circuit illustrated in the schematic shown in Figure 1.

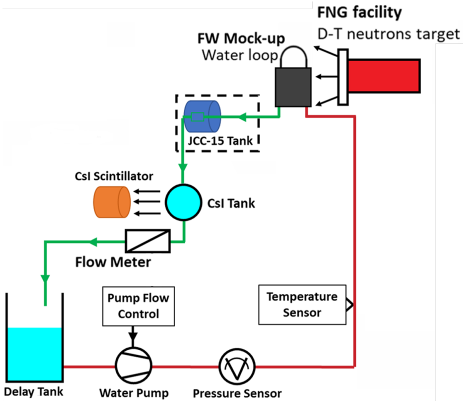

Figure 1: Schematic drawing of the N-16 experimental flowing water circuit at the FNG, circuit #1 (excluding dashed box) consists of the mock-up connected to the CsI tank and the delay tank, whereas circuit #2 also includes the JCC-15 tank in the dashed box.

A CsI detector was used to measure the gamma emission from N-16 and is described in Section 3.1, while a JCC-15 detector was used to measure the neutron emission from N-17 and is described in detail in Reference [5]. Two versions of the water circuit were used during the FNG experiment, for circuit #1 the FW mock-up was connected directly to the CsI in-line water expansion tank (referred to as the CsI tank), whereas for circuit #2 the FW mock-up was connected to the an in-line water expansion tank located inside the He-3 neutron detector ring (referred to as the JCC-15 tank and indicated in the dashed box in Figure 1), the JCC-15 tank was then connected to the CsI tank. Having two versions of the circuit provided more comprehensive experimental data to test the capabilities of the GamMaFlow code, a tool developed in Python and make sure the systems were modelled correctly. For both versions of the water circuit 1.8 m of plastic tubing (internal diameter 11 mm) connected the CsI tank with volume 0.1831 litres to the 110 litre delay tank. Inside the delay tank a pump circulated the water through 18.4 m of plastic tubing (internal diameter 28 mm) to the FW mock-up. In circuit #1 17.4 m of plastic tubing (internal diameter 11 mm) connected the mock-up to the CsI tank. Whereas in circuit #2 17.4 m of plastic tubing (internal diameter 11 mm) connected the mock-up to the JCC-15 tank with a water volume of 1.4223 litres, and 1 m of plastic tubing (internal diameter 11 mm) connected the JCC-15 tank to the CsI tank. The reduced internal diameter of the plastic tubing from the mock-up to the delay tank (green line in Figure 1) is to reduce the transit time between irradiation and detection. The CsI expansion tank was made from aluminium, with a wall thickness of ~0.5 cm to support the water pressure, the purpose was to increase the total activity that is present in the region of the detector and hence the count rate by increasing the volume of activated water seen by the CsI detector, the volume of the expansion tanks was optimised prior to the experimental campaign. The purpose of the water delay tank was to ensure that the N-16 nuclides had decayed extensively before the water was pumped back to the mock-up, where the irradiation-measurement cycle restarts. The results for N-17 have not been considered in this paper, but are presented in Reference [5].

2.1. Experimental procedure

The first stage was to set the water pump to frequencies between 10-50 Hz, in steps of 5 Hz, without the presence of neutrons. For the four experimental scenarios (circuit #1 with the mock-up at 5 cm and 2 cm, and circuit #2 with the mock-up at 5 cm and 2 cm) nine different flow rates were set, a more detailed description of the experimental procedure can be found in Reference [6]. With the mock-up at 5 cm the net count rate after background subtraction was predicted to be very low for the neutron detector but high for the CsI gamma detector, moving the mock-up to 2 cm would increase the net count rate in the neutron detector for the same FNG neutron yield but could saturate the CsI detector. Therefore, taking measurements at both distances optimised the results for both nuclides. Once the water flow rate had stabilised the deuteron beam was directed onto the FNG target to produce neutrons with a typical emission rate in the range of 1.3-2.0$\times10^{10}$ neutrons/s for typical irradiation times of 150-300 seconds. Here the experimental results have been normalised to 1×10^{10} neutrons/s so that direct comparisons can be made with calculated results. The time-of-flight (TOF) between the FW mock-up and the CsI tank was derived from the profile of the count rate vs time, as illustrated in Figure 2. When activated water reaches the CsI tank there is a sharp rise in the count rate, and there is a change in gradient observed on this rise. The first part of the rise is the result of partially activated water reaching the CsI detector, the change in gradient indicates the arrival of water that has passed through the full mock-up volume and experienced the full irradiation. The flow rate, calculated by dividing the sum of the volumes of the water from the FW mock-up by the TOF, was used to calculate the transit time through the FW mock-up using:

$$\text{transit time} = \frac{0.322}{\text{water flow}}, \quad (3)$$

where 0.322 litres is the volume of the FW mock-up.

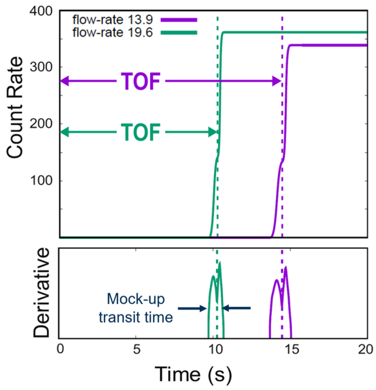

Figure 2: A plot to indicate the methodology used to calculate the TOF. The green and purple curves in the top plot show the activity build-up in the CsI tank for water flow rates 13.9 litres/min and 19.6 litres/min respectively for the ENDFB7.0 nuclear data library, with the mock-up positioned at 2 cm. The bottom plot shows the first derivative of the top plot, and the central dip indicates the TOF between the mock-up and the CsI tank.

3. Neutron transport and activation calculations

To calculate N-16 and N-17 reaction rates a well-characterised MCNP model of the FNG facility was integrated with a model for the FW mock-up created from the technical drawings provided by ENEA, illustrated in Figure 3 where the FNG model is shown in green, the mock-up in blue and the water in purple. The CAD model was converted into MCNP geometry and run using MCNP6.1. The water is assumed to be free of impurities with a natural abundance of oxygen. FENDL3.1d [7] cross-sections were used for all material definitions which included stainless steel for the tubes, AISI316LN for the body and CuCrZr for the section facing FNG target, detailed material compositions for the mock-up were provided by F4E in Reference [8]. During the experiment at ENEA aluminium struts were used to support the FW mock-up in-front of the FNG, the addition of a representative aluminium block behind the mock-up in the MCNP model resulted in a total percentage difference of N-16 atoms produced per source neutron per cm^3 across the full mock-up of <0.34%

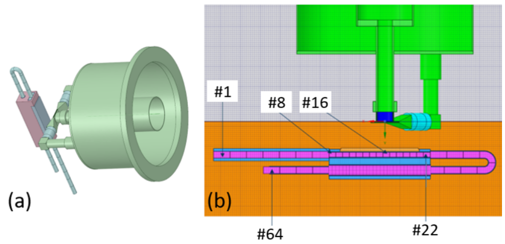

Figure 3: (a) shows a 3D model of the FNG (in green) and the FW mock-up (in purple and blue), (b) a CAD image showing the subdivision of the water regions inside the mock-up with some of the water element numbers indicated.

and therefore detailed modelling of the aluminium struts was not included in the final MCNP model.

In the CAD model the water inside the mock-up was subdivided into elements of roughly equal volume (~5 cm^3), a couple of elements on the bend of the mock-up were difficult to split and therefore varied by up to one significant figure. This was to enable the reaction rates to be determined for the water in the mock-up as a function of position and also to feed into the GamMaFlow code [9]. This slight variation in the volume of some of the elements has a negligible effect in comparison with the uncertainty on the measured volume of the mock-up, at 0.6%. The ^{16}O(n,p)^{16}N reactions rates were calculated in FISPACT-II using EAF-2010, TENDL2014, ENDFB7.0, JEFF3.2, and JENDL4, and in MCNP using ENDFB7.1, FENDL3.1d, FENDL2.1, FENDL3.0, ENDFB7.0, and JEFF3.3. In MCNP all calculations were run for 1×10^7 histories to reduce the statistical error in the reaction rates to less than 1% for each cell, with all cells passing the statistical tests in MCNP indicating convergence. The reaction rates per source neutron calculated for N-16 in each element of the mock-up component, with the mock-up positioned at 5 cm and 2 cm, are displayed in Figures 4 and 5, respectively. In MCNP the N-16 cross-section in each library all originated from ENDFB7, and therefore generated the same reaction rate values, therefore only one library for MCNP has been considered from this point. Figures 4 and 5 show the peak reaction rate in element 18 is 2.03×10^{-6} N-16 atoms per source neutron per cm^3 and 6.18×10^{-6} N-16 atoms per source neutron per cm^3, respectively.

The FW mock-up pipe element reaction rates from MCNP and FISPACT-II were used as input to the GamMaFlow code, which provides a temporal step-wise approach for simulating flowing water systems and evaluating inventory within different regions of a water circuit. The tool assumes the system consists of straight

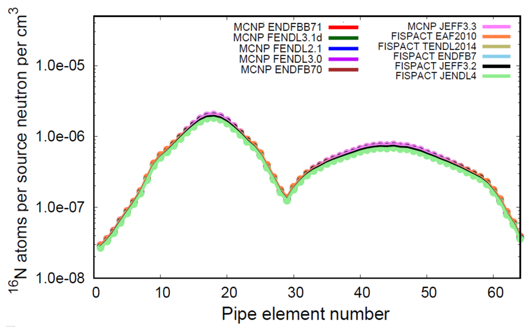

Figure 4: Reaction rates per element for N-16 derived inside the mock-up component, at 5 cm from the FNG source, using MCNP6.1 and FISPACT-II.

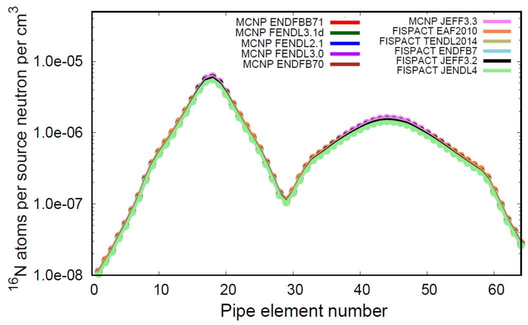

Figure 5: Reaction rates per element for N-16 derived inside the mock-up component, at 2 cm from the FNG source, using MCNP6.1 and FISPACT-II.

cylindrical pipes with sections of variable radius, and laminar flow with no radial velocity. The methodology involves subdividing the water circuit into cylindrical elements of equal size and transporting water along the pipe in discrete time steps. When the water element is within a defined neutron irradiation region N-16 atoms are created and added to the inventory for that pipe element. The code also tracks the decay of N-16 atoms as the water moves through the circuit.

3.1. CsI detector modelling

A large CsI scintillator (~25 cm diameter and ~20 cm height) coupled to a photo-multiplier tube was used to measure the gamma-lines from N-16. The CsI detector was placed behind a 1 m thick concrete shielding wall ~15 m from the FNG source to shield from neutrons, and was surrounded by a 5 cm thick copper layer and 10 cm of lead to reduce background noise. A detailed MCNP model of the CsI detector was provided by ENEA, and included the CsI tank containing a wedge-shaped deflector (to enable water mixing within the expansion tank) that was placed 13.5 cm from the CsI detector end-cap, as shown in Figure 6.

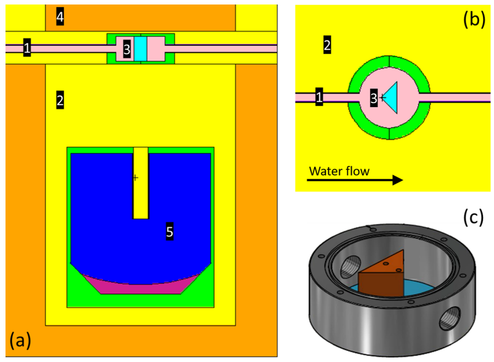

Figure 6: MCNP model showing (a) PZ = 0 slice of the CsI detector and CsI expansion tank and (b) PY = 14 slice of the CsI expansion tank (c) CsI expansion tank taken from the CAD drawing. In (a) and (b) label 1 indicated the water pipes, 2 indicates regions of air, 3 shows the CsI water expansion tank with an aluminium wall in green and deflector wedge in turquoise, 4 indicates the copper shield in orange (lead not shown), and 5 shows the CsI detector crystal in blue (with the dead-layer in purple). The direction of water flow is indicated in (b).

The experimentally measured energy resolution of the CsI was incorporated in MCNP using the Gaussian Energy Broadening (GEB) function. Using this the efficiency of the CsI detector between 5.5-6.5 MeV (corrected for the branching ratio) was calculated to be 2.32%, this included contribution from the inlet and outlet pipes as well as the water inside the expansion tank, the probability of emission from these three regions was given as the ratio of the activities.

4. Results

The preliminary results from the calculations and the experimental campaign, as well as C/E values and uncertainties, are presented in Table 1. The calculated CPS values were obtained by multiplying the activity at the CsI detector output from GammaFlow with the CsI detector efficiency and branching ratio. The experimental CPS values were obtained from the count rate in 5.5-6.5 MeV energy region, after background subtraction. The uncertainties in the C/E values have been summed in quadrature and consider a 10% contribution from the nuclear data libraries [10], 5% uncertainty in the efficiency of the CsI detector from the calibration and detector modelling [11], 4% for the evaluation of the FW mock-up neutron flux, 0.9-5% uncertainty on the TOF (the higher the water speed the higher the uncertainty), 0.6% uncertainty from the FW mock-up volume.

Table 1: C/E values with uncertainties calculated for different flow rates, for circuit #1 and #2 with the mock-up positioned at 5 cm and 2 cm. A TOF comparison between experimental values and values calculated using GammaFlow is also presented.

		Pump frequency (Hz)	Flow rate (litre/min)	TOF through mock-up (s)	TOF to CsI detector (s)		Calculated CPS	Experimental CPS	C/E	Error ±
					Experimental	Calculated				
Circuit #1	Mock-up at 5 cm	10	10.2	1.894	10.7	10.8	1822	1993	0.91	0.11
		15	16.3	1.186	6.7	6.8	1716	1922	0.89	0.11
		20	21.8	0.885	5.0	5.1	1525	1697	0.90	0.11
		25	27.3	0.708	4.0	4.0	1350	1507	0.90	0.11
		30	34.1	0.566	3.2	3.2	1173	1344	0.87	0.11
		35	39.0	0.496	2.8	2.8	1069	1228	0.87	0.11
		40	43.7	0.443	2.5	2.5	984	1125	0.87	0.11
		45	49.6	0.389	2.2	2.2	893	1031	0.87	0.11
		50	54.6	0.354	2.0	2.0	829	948	0.87	0.11
	Mock-up at 2 cm	10	10.1	1.912	10.8	10.9	3294	3361	0.98	0.12
		15	16.0	1.204	6.8	6.9	3128	2982	1.05	0.13
		20	21.8	0.885	5.0	5.1	2765	2684	1.03	0.12
		25	27.3	0.708	4.0	4.0	2449	2382	1.03	0.12
		30	34.1	0.566	3.2	3.2	2128	2121	1.00	0.12
		35	37.6	0.513	2.9	2.9	1990	1924	1.04	0.13
		40	43.7	0.443	2.5	2.5	1785	1757	1.02	0.13
		45	47.5	0.407	2.3	2.3	1676	1578	1.06	0.13
		50	52.0	0.372	2.1	2.1	1563	1492	1.05	0.14
Circuit #2	Mock-up at 5 cm	10	13.3	1.448	15	15.1	928	1000	0.93	0.11
		15	19.2	1.004	10.4	10.5	1020	1168	0.87	0.10
		20	25.0	0.772	8.0	8.0	998	1131	0.88	0.11
		25	29.4	0.656	6.8	6.8	956	1065	0.90	0.11
		30	37.1	0.521	5.4	5.4	873	1002	0.87	0.11
		35	41.7	0.463	4.8	4.8	824	935	0.88	0.11
		40	45.5	0.425	4.4	4.4	786	886	0.89	0.11
		45	52.7	0.367	3.8	3.8	721	836	0.86	0.11
		50	58.9	0.328	3.4	3.4	671	789	0.85	0.11
	Mock-up at 2 cm	10	13.9	1.390	14.4	14.5	1717	1576	1.09	0.13
		15	19.6	0.984	10.2	10.3	1851	1895	0.98	0.12
		20	25.7	0.753	7.8	7.8	1799	1917	0.94	0.11
		25	30.3	0.637	6.6	6.6	1717	1873	0.92	0.11
		30	37.1	0.521	5.4	5.4	1583	1774	0.89	0.11
		35	43.5	0.444	4.6	4.6	1462	1666	0.88	0.11
		40	47.7	0.405	4.2	4.2	1388	1600	0.87	0.11
		45	52.7	0.367	3.8	3.8	1308	1494	0.88	0.11
		50	64.6	0.299	3.1	3.1	1144	1409	0.81	0.10

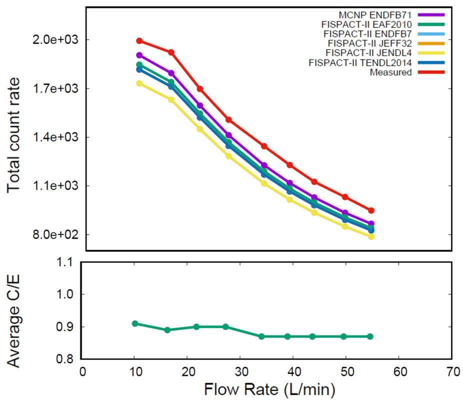

Figure 7: The total count rate calculated for N-16 in the CsI detector with the mock-up at 5 cm for circuit #1 at various water flow rates.

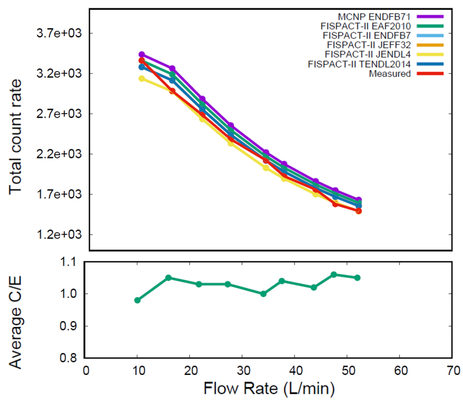

Figure 8: The total count rate calculated for N-16 in the CsI detector with the mock-up at 2 cm for circuit #1 at various water flow rates.

5. Discussion and conclusions

A water activation experiment was performed at the 14 MeV Frascati Neutron Generator to validate the methodology for water activation assessment used for ITER and to provide scientific justification to reduce safety factors. This paper has provided a comparison of

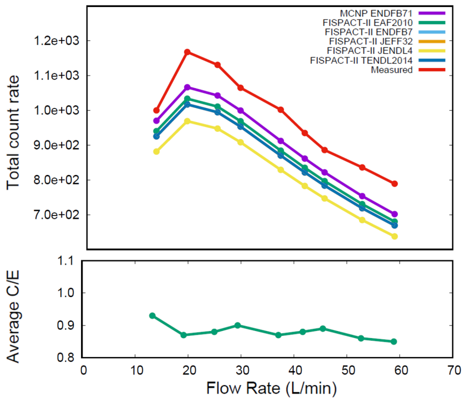

Figure 9: The total count rate calculated for N-16 in the CsI detector with the mock-up at 5 cm for circuit #2 at various water flow rates.

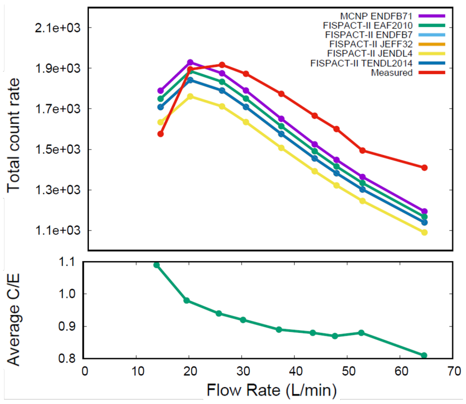

Figure 10: The total count rate calculated for N-16 in the CsI detector with the mock-up at 2 cm for circuit #2 at various water flow rates.

experimentally measured activities of N-16 with simulated results. Reaction rate data was extracted for ten nuclear data libraries using MCNP6.1 with pointwise libraries and FISPACT-II with group-wise libraries, although the data from the libraries used with MCNP originated from ENDFB7, therefore only effectively five libraries were compared. The water inside the FW mock-up was subdivided into elements of roughly equal volume. Relatively good agreement was found between the various nuclear data libraries EAF-2010, TENDL-2014, ENDFB7, JEFF3.2 and JENDL-4, with a factor of 1.12 and 1.11 in reaction rate between the highest and lowest values for element 18, with the mock-up at 5 cm and 2 cm respectively.

The reaction rates provided input to the GammaFlow code, which was used to track the movement of the activated water through the complex irradiation and flow volume cases, to provide an estimation of the activity of N-16 at the CsI tank and to provide direct comparison with experimental data. One of the aims of this work was to validate the GammaFlow code using experimental data. The data provided in Table 1 shows a comparison in the calculated and measured TOF between the FW mock-up and CsI tank, with an average percentage difference of 0.77% showing excellent agreement with measured TOF values and suggesting the water circuit was well-defined in the GammaFlow code compared with the experimental setup at ENEA. Although there is a tendancy to underestimate the activity for water flow rates exceeding 10 litres/minute, this could originate from the GammaFlow code and the fact that water mixing is not considered in this work.

The activities calculated in the CsI tank using the GammaFlow code were corrected for CsI detector efficiency and branching ratio to provide the final experimental CPS values presented in Table 1, and used to calculate the C/E values. The overall C/E value averaged over the four measurement scenarios was 0.93±0.11, which shows good agreement with the simulated results.

6. Acknowledgements

The UKAEA were subcontracted by ENEA to complete this work which was funded by Fusion from Energy under the Contract F4E-OPE-0956. This publication reflects the views of the authors only, and Fusion for Energy cannot be held responsible for any use which may be made of the information contained therein. The views and opinions expressed herein do not necessarily reflect those of the ITER Organization.

References

[1] https://www.nndc.bnl.gov (accessed: 14/03/2019).
[2] https://www-nds.iaea.org (accessed: 04/03/2019).
[3] Calculation of activation water radiation maps in ITER, Neutronics Challenges of Fusion Facilities-II,, Transactions of the American Nuclear Society, 116, 2017.
[4] Nuclear Analysis of 16N and 17N radiation fields from TCWS activated water, IDM Number: ITER_D_QZ7BEK_v2.1, 16/11/2016.
[5] M. Angelone, et al., Measurements of delay neutron emission from water activated by 14 MeV neutrons in a FW mock-up of ITER, preprint submitted to ISFNT, 2019.
[6] M. Pillon, et al., Comparison between measurement and calculations for a 14 MeV neutron water activation experiment, preprint submitted to ND2019, 2019.
[7] *FENDL-3.1d: Fusion Evaluated Nuclear Data Library Ver.3.1d*, [Online]. Available: https://www-nds.iaea.org/fendl/index.html (2018).
[8] Maquette B1 (OPE-097) Material Properties (2G8B99 v1.0).
[9] C.R.Nobs, GammaFlow Code Development at UKAEA (memo), doc. ref. GammaFlow.issue1 (2019).
[10] EAF-2010 Nuclear Data Library. Available: https://www.oecd-nea.org/dbforms/data/eva/evatapes/eaf_2010/ (2011).
[11] M. Pillon, Private communication (04/10/2017).